

ASKAP Array Configurations: Technical Studies

Neeraj Gupta, Simon Johnston & Ilana Feain
Australia Telescope National Facility, CSIRO

August 8, 2008

Abstract

In this document we explore the possibilities for different array configurations for the Australian Square Kilometre Array Pathfinder (ASKAP) based on the requirements of the science case (Johnston et al. 2007). The configurations are constrained by the land available at the Murchison Radio Observatory, a mask of unsuitable locations within the site, and the budget for the backend computing.

We concentrate on options available for a 45 antenna system. We present optimised configurations resulting in a 60'', 30'' and 10'' synthesised beam, spatial scales which are most suitable for low-surface brightness science, an extragalactic HI emission survey and a continuum survey respectively. We then examine various hybrid and scale-free options in an attempt to provide an array suitable for all science cases.

We show that a hybrid configuration optimised for two spatial scales (10'' and 30'') returns an equivalent sensitivity of $\sim 75\%$ compared to the optimum configurations. A scale-free array provides a sensitivity of $\sim 50\text{-}60\%$ over three spatial scales (10'', 30'' and 60'') but has significantly poorer sidelobe levels.

The options and recommendations arising from this study are given in a companion paper (Feain et al. 2008).

1 Introduction

The system parameters and science case for ASKAP were presented in Johnston et al. (2007). Seven headline science goals were listed; three of these seven made demands on the telescope configuration as outlined below. Furthermore, 30 antennas is seen as the minimum possible to do the science required over the finite lifetime of ASKAP and 45 antennas is declared as the target goal.

- **The detection of a million galaxies in atomic hydrogen:** The optimum configuration for this survey would result in a synthesised beam of $\sim 30''$ and an excellent point spread function to obviate the need for deconvolution (see Staveley-Smith 2006).
- **The detection of synchrotron radiation from 60 million galaxies:** This continuum survey requires high resolution to avoid confusion but also needs surface brightness sensitivity to avoid filtering out nearby galaxies. Achieving a dynamic range in excess of 10^4 is required. Condon (2008) has argued that the optimum resolution for ASKAP would be $\sim 10''$.
- **Understanding the interstellar medium of our own galaxy and mapping the cosmic web:** These surveys require high low surface brightness sensitivity resulting in a beam greater than $\sim 1'$.

Each of these surveys would expect to take at least one full year of telescope time to achieve its science goals, even when operating at full sensitivity. The challenge for configuration studies is therefore to devise a configuration capable of satisfying the science goals whilst maintaining sensitivity over a wide range of spatial scales.

In this paper, we present various options for the array configurations that are available for ASKAP consisting of 45 antennas. In Section 2, we describe the land available at Murchison Radio Observatory site. In Section 3 we describe the method used for optimising array configurations. In Section 4, we show that with 45 antennas it is possible to obtain the configurations that will be suitable for extragalactic HI emission and continuum surveys and low-surface brightness science. In Section 5 we present the hybrid configurations where resolutions suitable for ASKAP HI and continuum surveys can be obtained by reweighting the visibilities. These results are also compared with 45 antenna scale-free configurations. In Section 6 we summarise the results for the different configurations and their impact on ASKAP surveys.

2 Site and site mask

ASKAP is planned to be located on the Murchison Radio Observatory (MRO) in inland Western Australia, one of the most radio-quiet locations on the Earth and one of the sites selected by the international community as a potential location for the SKA. The approximate geographical coordinates of the site are longitude 116.5 east and latitude 26.7 south. The site mask (see Fig. 1) is derived from (a) a comprehensive environmental assessment of the site (Alexander Holm and Associates 18 Jan 2008) and conforms to all recommendations within that assessment, and (b) a heritage survey by archaeological and anthropological consultants along with the local indigenous group, which focussed on the central portion of the polygon. Further small changes to the site mask may still be required.

3 Optimisation Method

We solve for array configurations i.e. antenna locations by specifying a model visibility distribution (V_M). V_M is defined by the desired resolution i.e. psf and sidelobe levels. The configuration problem is then reduced to determining antenna locations consistent with the terrain constraints of telescope site such that model visibility distribution is realised for the specified observational set-up. Here, the observational set-up is essentially defined by site latitude, source declination, frequency, fractional bandwidth, number of channels and hour angle (HA) coverage. The configuration problem and basic algorithm to obtain the antenna locations optimised for the V_M are described in Boone (2001) and Keto (1997) (see also Cornwell (2006)). In short, for a given antenna layout initial visibility distribution (V_I) is compared with V_M to determine the pressure forces on visibility samples. These pressure forces are then used to iteratively move the antenna locations so as to eventually realise V_M . de Villiers (2007) presented an efficient method for optimizing array layout without the need for gridding the visibility data points and estimating a 2-dimensional density function. Software `AntConfig` written by Mattieu de Villiers is based on this novel algorithm. We use `AntConfig` to obtain the antenna configurations optimised for different observing set-ups and compare the properties of these arrays in visibility and image plane using tools in Common Astronomy Software Application (CASA)¹.

Configuration problem for ASKAP requires solving for arrays which will

¹CASA is distributed by National Radio Astronomy Observatory (NRAO).

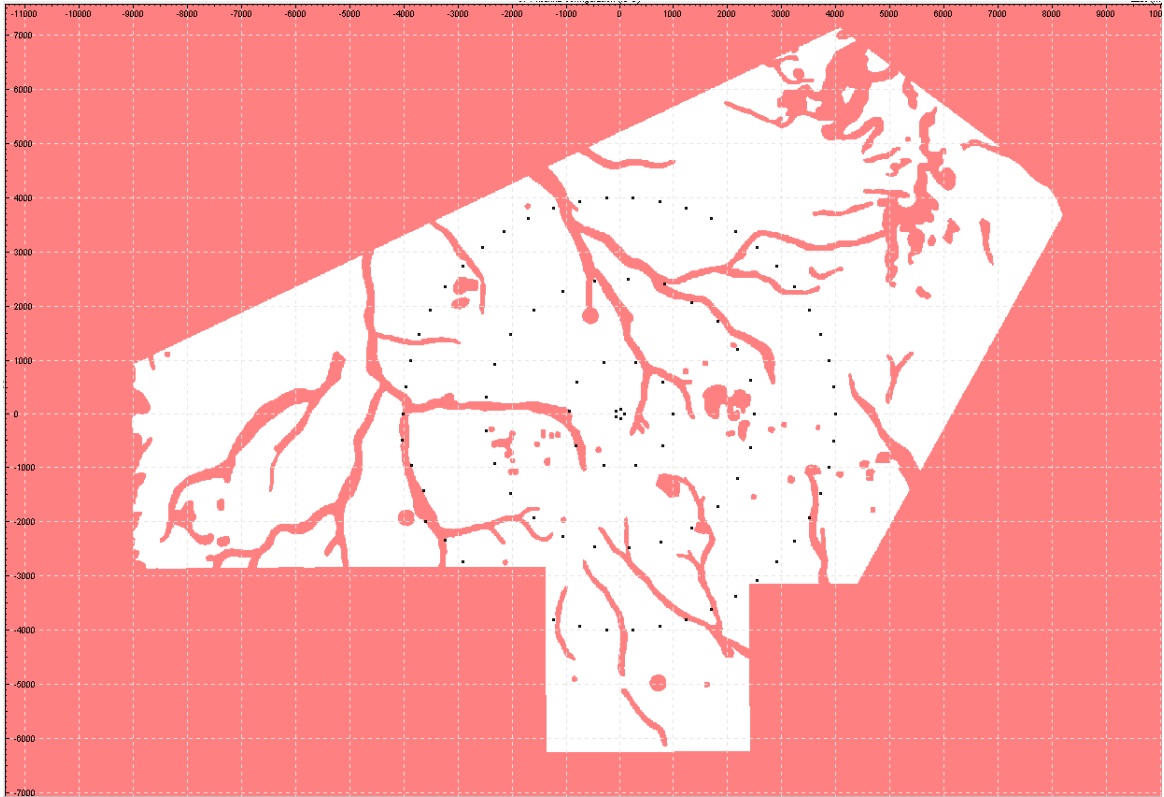


Figure 1: Mask of the MRO site. The sides of the box are 15×21 km in length and each small square is 1000 m on the side. Shaded (pink) regions denote areas either outside the boundaries or those forbidden by the site mask. Also shown are circles with diameter 200, 500, 2000 and 8000 m.

have good psfs of $10''$, $30''$ and $1'$. We refer to these as Long, Medium and Compact configuration respectively. Arrays optimised for $30''$ and $1'$ must have very low sidelobe levels of only a few percent. This is required for the HI emission surveys (Galactic and extragalactic) for which images will not be deconvolved to keep the computing load within manageable limits. The arrays must also have good snapshot uv coverage. In the following we show that it is indeed possible to obtain the configurations with 45 antennas that satisfy the above criterion and will be suitable for surveys envisaged for ASKAP.

4 Single scale configurations

4.1 Configurations optimised for HI emission surveys

The ASKAP extragalactic HI emission survey requires a good psf of $\sim 30''$. Due to enormous computing load images for this survey will not be deconvolved. So it is essential that sidelobe levels of the psf be no more than a few percent (Staveley-Smith 2006). An array configuration where 45 antennas are arranged to give Gaussian distribution of visibilities with a scale of about 700 m will give the best results. Such an array will not only have a good psf but will also make use of the sensitivity of all the antennas. This is highly desirable as the HI emission survey is sensitivity limited.

To obtain the configurations suitable for this we set parameters baseline sigma and maximum baseline to 700 and 2500 m respectively. This sets the V_M to be a Gaussian corresponding to FWHM of $\sim 30''$ in image plane. A smaller value of maximum baseline would result in arrays which are similar to circular ring and are undesirable in this case as they will have higher sidelobe levels. Simulations were done at observing frequency of 1.4 GHz. Configurations were obtained for sources at the declinations of 10 , -10 , -30 , -50 , -70 and -90 degrees. For each of these, optimisation was done for a observing runs of 4, 8 and 12 hrs². Final results were also compared with the snapshot³ observing run. This allowed us to explore the parameter space completely and also test the stability of optimisation. Performance of each of these arrays in the image and visibility plane was then tested using tools in CASA. Arrays were compared for the robustness of psf (FWHM as well as sidelobes) for the sources at different declinations. In general we found that arrays optimised for 4 or 8 hrs observing run performed better than the

²Observing runs were centered at 0 hour angle.

³Snapshot mode lasted 12 mins.

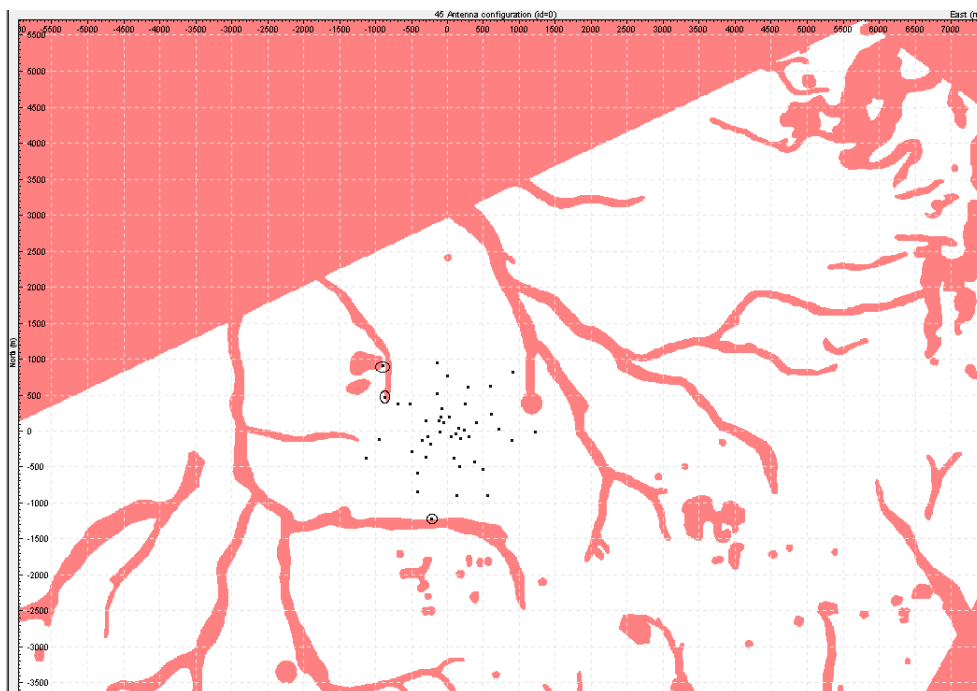


Figure 2: Layout of 45 antennas for the ASKAP H₁ (Medium) array.

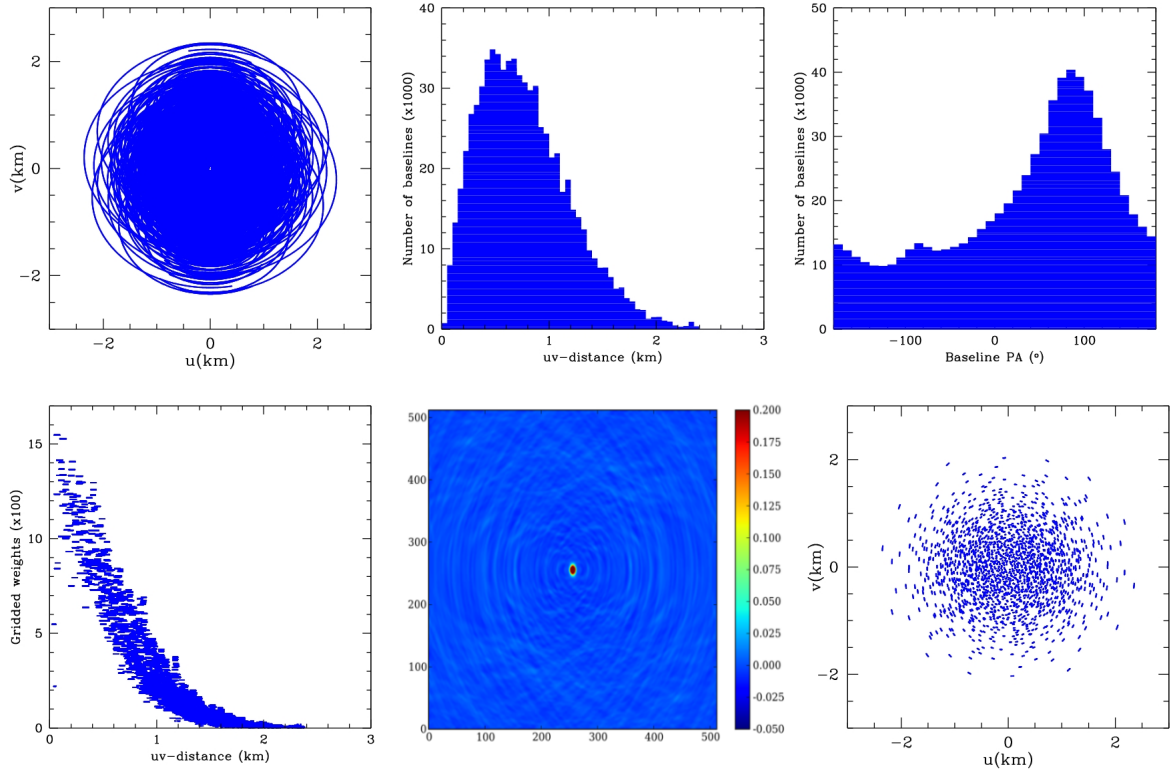


Figure 3: Properties of the (Medium) array configuration given in Fig. 2. The antenna spacing for the array ranges from 59 m to 2.4 km. *Top*: uv-coverage, distribution of baselines and baseline position angles for the observing run from HA -6 to $+6$ hrs with source at declination of -50° . *Bottom*: Gridded weights and psf ($30'' \times 24''$) corresponding to the same. Snapshot uv-coverage is also shown.

arrays optimised for 12 hrs as latter had lesser number of shorter antenna spacings.

Of all the arrays tested we find that the one shown in Fig. 2, optimised for a 4 hrs run with source at declination of -30° , is best in terms of psf sidelobes and its robustness for the sources at different declinations. It has antennas randomly distributed and has more short baselines compared to other arrays (see Fig. 2). Properties of this array in visibility and image planes are shown in Fig. 3 for a 12 hrs long observing run. Clearly uv-coverage is good and sidelobe levels for the psf shown in same figure are in the range: $(-1.1\%, 1.3\%)$. Such an array will be suitable for the HI emission survey and will also have good snapshot imaging properties. It is interesting to estimate the sensitivity of this array for a psf of $2-3'$. Reweighting the visibilities for 12 hrs run shown in Fig. 3 we find that array will have only 15% sensitivity for the tapered beam of $3'$.

4.2 Configuration optimised for Continuum surveys

Resolution required for the continuum surveys planned with ASKAP is better than $\sim 10''$ so that the survey is not confusion limited (Condon 2008). The method followed to obtain the arrays suitable for this was the same as described above, except for the fact that V_M was set to have uniform coverage of baselines. This can be done by setting value of baseline sigma close to (or larger) than maximum baseline. We find that when this is done, resultant array has most of the antennas distributed along a perturbed ring. In Fig. 4, we present the best configuration that we obtained with baseline sigma and maximum baseline set to 6000 and 7500 m respectively. In Fig. 5, we show the 12 hrs and snapshot uv-coverage for this array (referred to as Long). Sidelobe levels for the 12 hrs observing run are in the range: $(-1.2\%, 4.1\%)$. Snapshot uv-coverage is also good. Given the shape and extent of ASKAP site, it is not possible to optimise the array configurations with baselines greater than ~ 8 km. Reweighting the visibilities for 12 hrs run shown in Fig. 5 we find that a psf of $30''$ can be obtained with about 80% loss in sensitivity.

4.3 Configurations optimised for low-surface brightness

In Fig. 6 we show the configuration optimised with baseline sigma and maximum baseline set to 200 and 500 m respectively. For this particular optimisation, source was taken to be at declination of -30° and optimisation was done for an observing run of 8 hrs. Such an array is required to achieve the

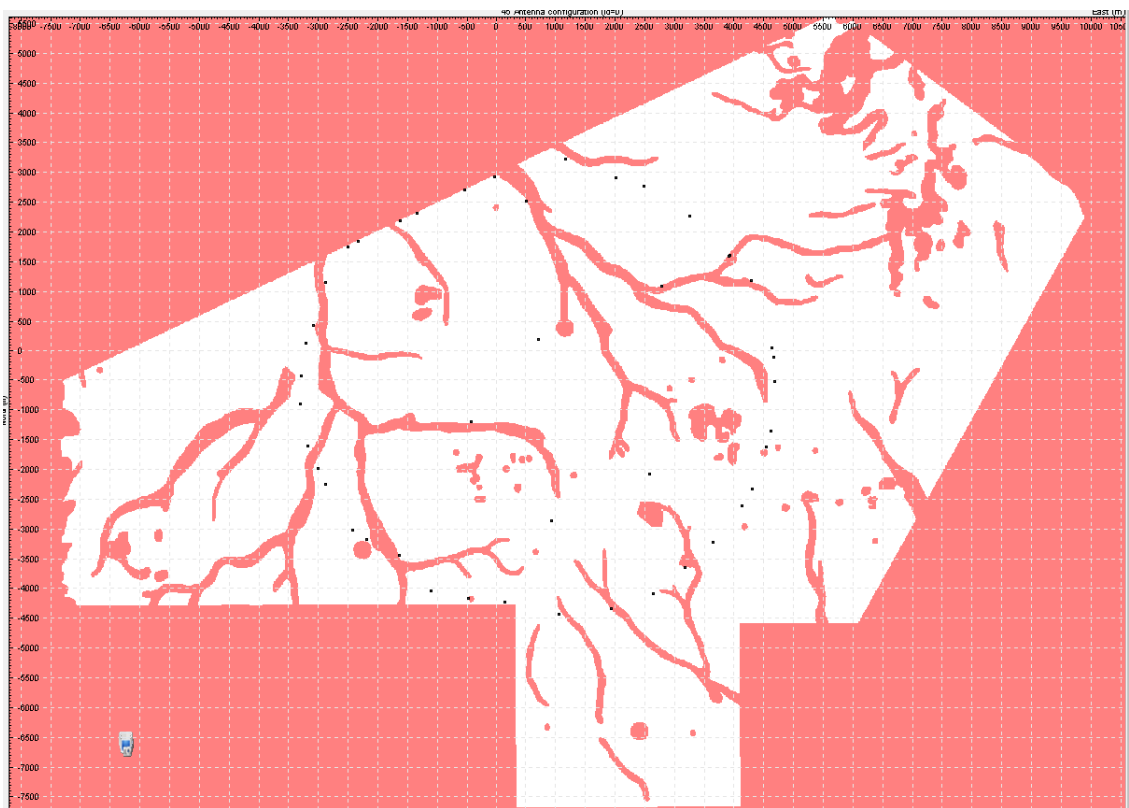


Figure 4: Layout of 45 antennas for ASKAP continuum (Long) array

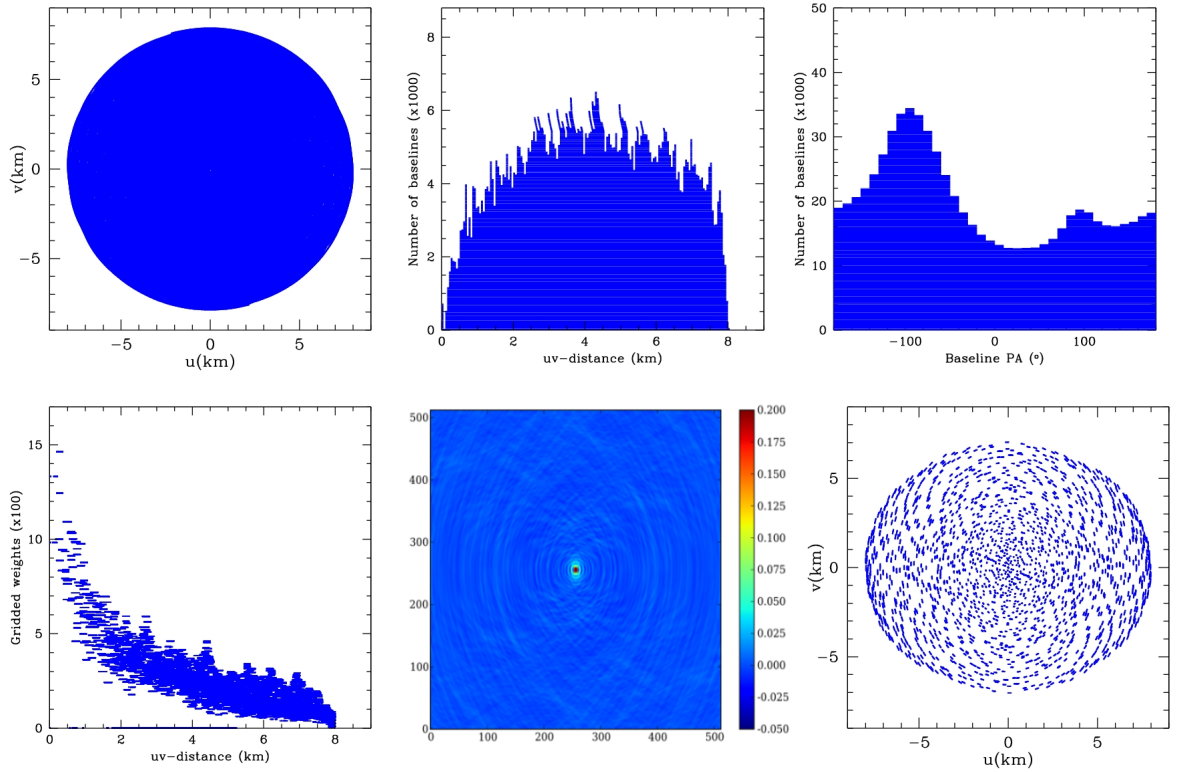


Figure 5: Properties of array configuration shown in Figure 4. Antenna spacing for the array ranges from 21 to 8000 m. *Top*: uv-coverage, distribution of baselines and baseline position angles for the 12 hrs observing run with source at declination of -50° . *Bottom*: Gridded weights and psf ($5'' \times 4''$) corresponding to the same. Snapshot uv-coverage is also shown.

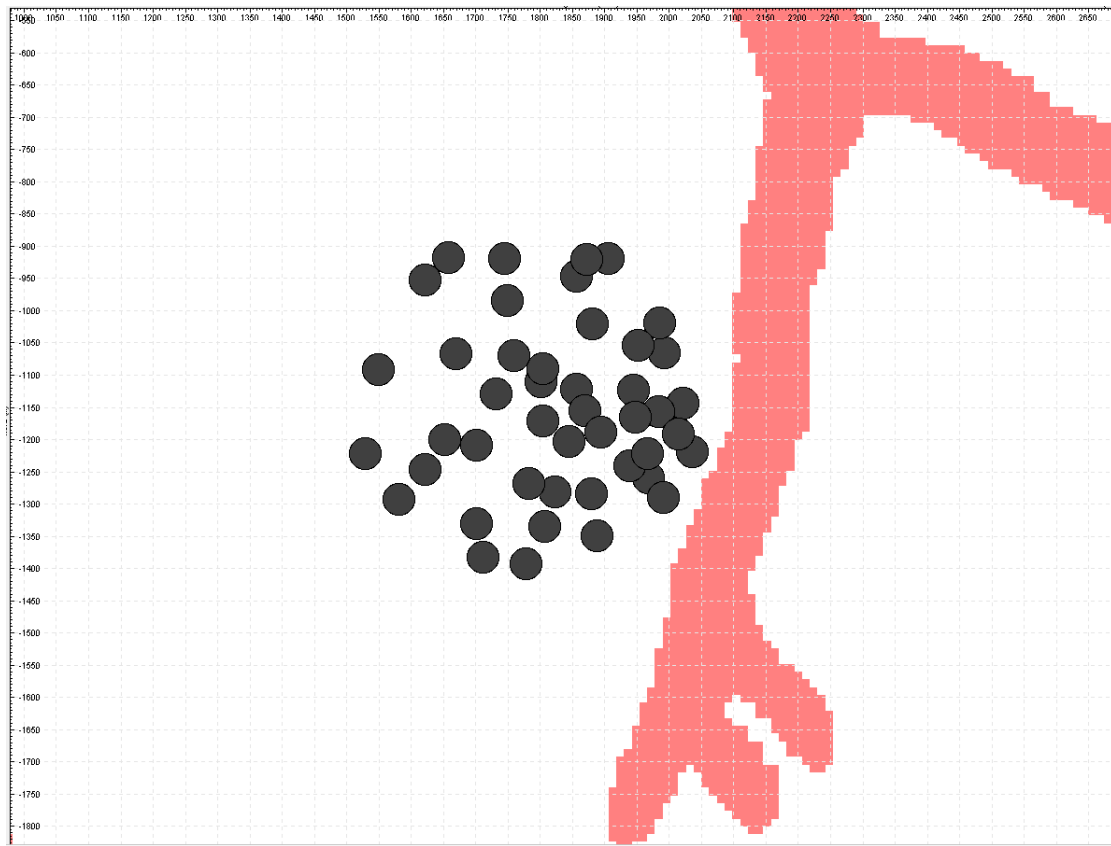


Figure 6: Layout of 45 antennas for the ASKAP (Compact) array suitable for the low-surface brightness science.

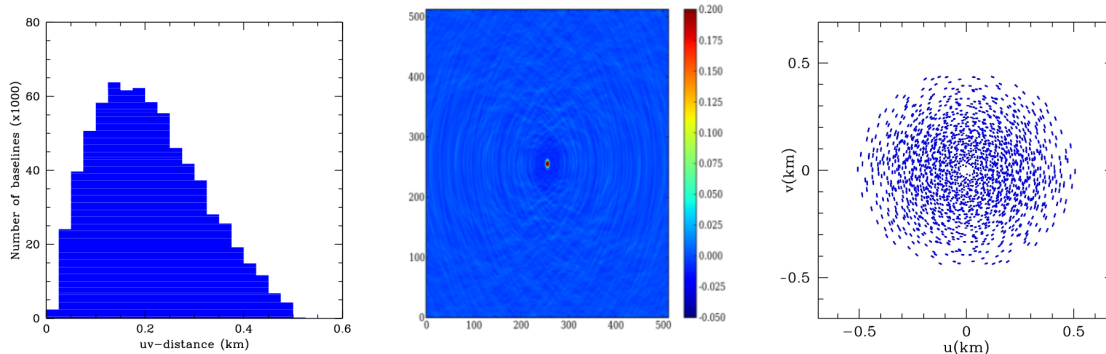


Figure 7: Properties of array configuration shown in Fig. 6. *Left*: Distribution of baselines for the 12 hrs observing run with source at declination of -50° . *Middle*: Point spread function ($111'' \times 87''$) corresponding to this baseline distribution. Sidelobe levels are in the range: $(-1.5\%, 1.1\%)$. *Right*: Snapshot uv-coverage.

low-surface brightness ASKAP science. In Fig. 7, we show the 12 hrs and snapshot uv-coverage for this array. Sidelobe levels for the 12 hrs observing run are in the range: $(-1.5\%, 1.1\%)$. Snapshot uv-coverage is also good.

5 Hybrid configurations

In the previous sections we explored 45 antenna configurations that were optimised for the requirements of either HI emission surveys, continuum surveys or low-surface brightness science. Realistically it is highly desirable that a single array configuration is obtained. In this section we consider the possibilities of such hybrid configurations for ASKAP. Our aim is to design the configuration from which good psfs of $10''$ and $30''$ by reweighting the visibilities such that sensitivity loss is as low as possible but no lower than 30%. To achieve this we arrange 45 antennas in the following configuration:

- Core of 33 antennas optimised for a Gaussian baseline distribution with a scale of 700 m. `AntConfig` parameters were chosen to be the same as for the optimisation of Medium configuration described in Section 4.
- Remaining 12 antennas arranged in the form of a perturbed ring of diameter 5 km. Antennas on the ring, by design, have separation

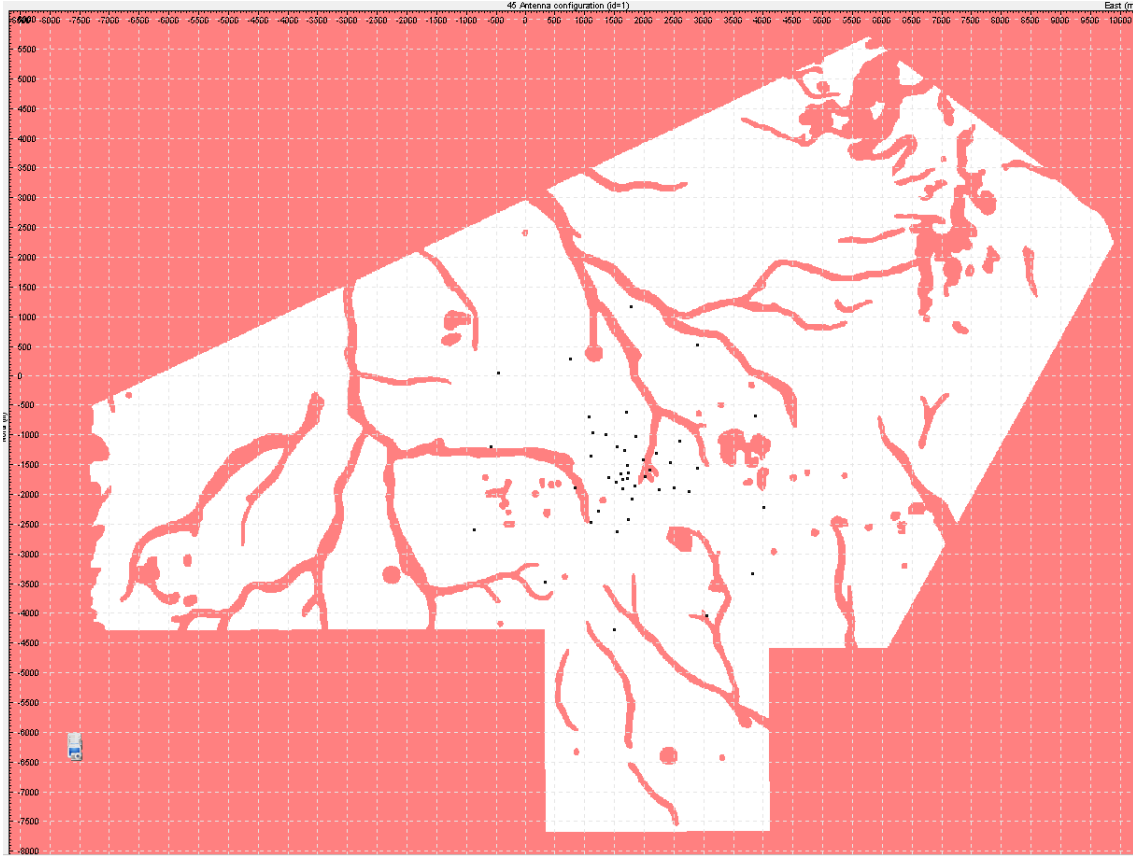


Figure 8: Layout of 45 antennas for ASKAP Hybrid array.

greater than ~ 1.3 km. This ring of antennas therefore produces a uniform coverage of baselines longer than ~ 1.3 km.

In Figs. 8 and 9, we show the layout of the antennas and properties of the array for a 12 hrs synthesis observing a source at -50° . This array by design has a sensitivity of 73% sensitivity for a psf of $\sim 30''$. Psf sidelobe levels are in the range: $(-1.3\%, 1.3\%)$. These numbers for $30''$ are for natural weighted data. Psf of $11.2'' \times 8.6''$ can be obtained by reweighting the visibilities shown in Fig. 9. Sidelobe levels are in the range: $(-3.3\%, 5.3\%)$ and $\sim 73\%$ of the total sensitivity is retained. Therefore this configuration provides imaging performance (in terms of sidelobe levels) that is as good as those in Figs. 2 and 4.

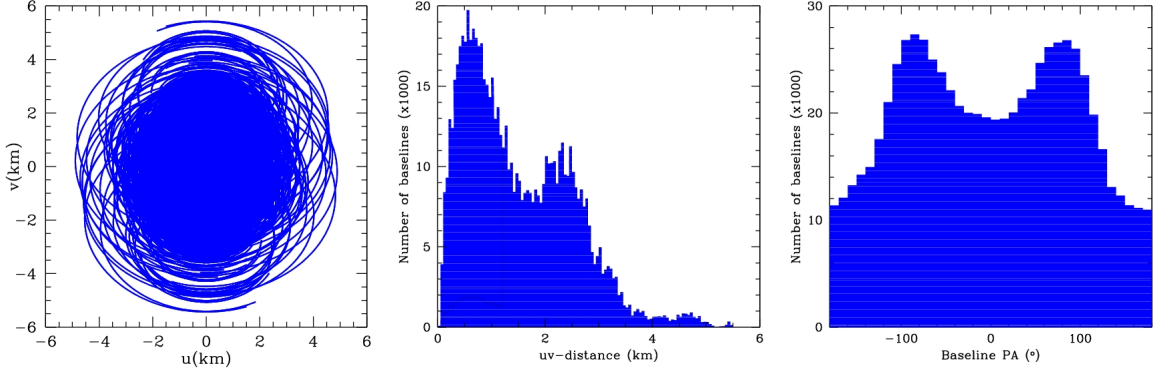


Figure 9: Hybrid array configuration. *Left*: uv-coverage for observing run from HA -6h to $+6\text{h}$ with source at declination of -50° . *Middle*: Distribution of baselines as function of uv-distance and *Right*: Distribution of baseline position angles as function of uv-distance. For the uv-coverage shown above, natural weighted psf is $15.9'' \times 12.0''$ and sidelobe levels are in the range: $(-1.3\%, 5.4\%)$.

5.1 Scale free configurations

Scale-free or self-similar configurations has often been proposed as arrays that have good sensitivity over a wide range of spatial scales. Here we compare the performance of such self-similar configurations with the configurations presented so far. For this purpose, we construct a set of self-similar configurations where a total of 45 antennas are placed on rings of radii increasing in geometric progression. Radius of the smallest ring comes from the number of antennas in each ring and the fact that shortest separation between any antennas be 25 m to prevent the loss due to shadowing of antennas. Ratio of the radii of successive rings then follows from the constraint that extent of array be no larger than 5 km. With these considerations following four configurations are of interest to us:

- **ConfigA**: 5 antennas placed on 9 rings. Radius of smallest ring, $R_s=21$ m and ratio of the radius of successive rings, $r=1.82$.
- **ConfigB**: 7 antennas placed on 6 rings. $R_s=29$ m and $r=2.44$.
- **ConfigC**: 9 antennas placed on 5 rings. $R_s=37$ m and $r=2.87$.
- **ConfigD**: 11 antennas placed on 4 rings. $R_s=44$ m and $r=3.85$.

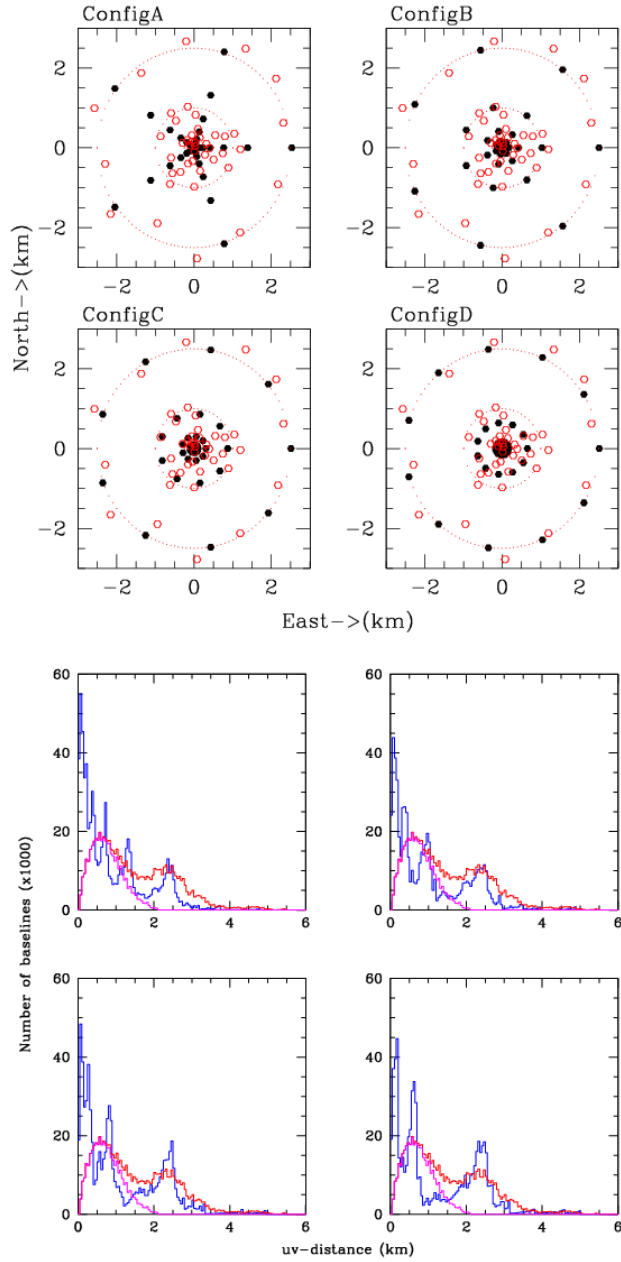


Figure 10: Self-similar configurations (black solid circles). Antennas for the hybrid configuration shown in Figure 9 are also shown as red open circles. 12 hrs baseline distribution for a source at -50° is also shown. Blue curve corresponds to scale-free configurations and red curve to the hybrid configuration. Also shown in magenta is the baseline distribution for 33 core antennas of the hybrid configuration in Figure 9.

Layout of antennas and uv-coverage for a 12 hrs synthesis with source at -50° for these configurations are shown in Fig. 10. Of all the self-similar configurations, **ConfigC** has baseline distribution most similar to that of the hybrid array in Figure 9. In the following we compare their performances. Shown in Fig. 11 are the natural weighted psfs for the hybrid array and **ConfigC**. Clearly, the psf of the hybrid configuration is far better than of **ConfigC** which has very high sidelobe levels. Next we consider the performance of these arrays when visibilities are reweighted to obtain a psf of $\sim 30''$. For this we reweight the visibilities of **ConfigC** in following two ways:

- **wt1**: Visibilities for **ConfigC** are weighted to make the effective baseline distribution similar to the baseline distribution for the core of the hybrid array.
- **wt2**: Same as **wt1** except that baselines shorter than 500 m are given substantial weights. We consider lack of baselines shorter than 500 m as the deficiency of the hybrid array. We aim to overcome this deficiency in the future designs of hybrid configurations. In order to measure the impact of these baselines for $30''$ psf we consider this weighting scheme here.

In Fig. 11, we show the effective baseline distributions and psfs for **ConfigC** after applying above mentioned weighting schemes. In general we find that sidelobe levels for **ConfigC** are at least worse by a factor 2 when compared with those of the hybrid array. For **wt1** and **wt2**, sensitivities for **ConfigC** are 56% and 61% respectively. It may be noted that the hybrid array (by design) has a sensitivity of $\sim 73\%$ for $\sim 30''$ psf. Next we reweighted (downweighting baselines shorter than 1200 m) visibilities for **ConfigC** to obtain a psf of $\sim 10''$. In this case, sensitivity retained is 61% and sidelobe levels for the psf ($11.0'' \times 8.5''$) are in the range: $(-9.8\%, 8.6\%)$. Again, both sidelobe levels and sensitivity are significantly better for the hybrid array. Performance of **ConfigB** for psf of $\sim 30''$ are similar to that of **ConfigC** but sensitivity achieved for the $\sim 10''$ is worse. On the other hand, **ConfigD** performs similar to **ConfigC** for $\sim 10''$ psf but sidelobe levels for the similar sensitivities are worse for $\sim 30''$ psf. Therefore, we conclude that for extragalactic HI emission and continuum surveys the hybrid array provides better sensitivities and imaging performance as compared to **ConfigC** (which is better as a whole than **ConfigB** and **ConfigD**).

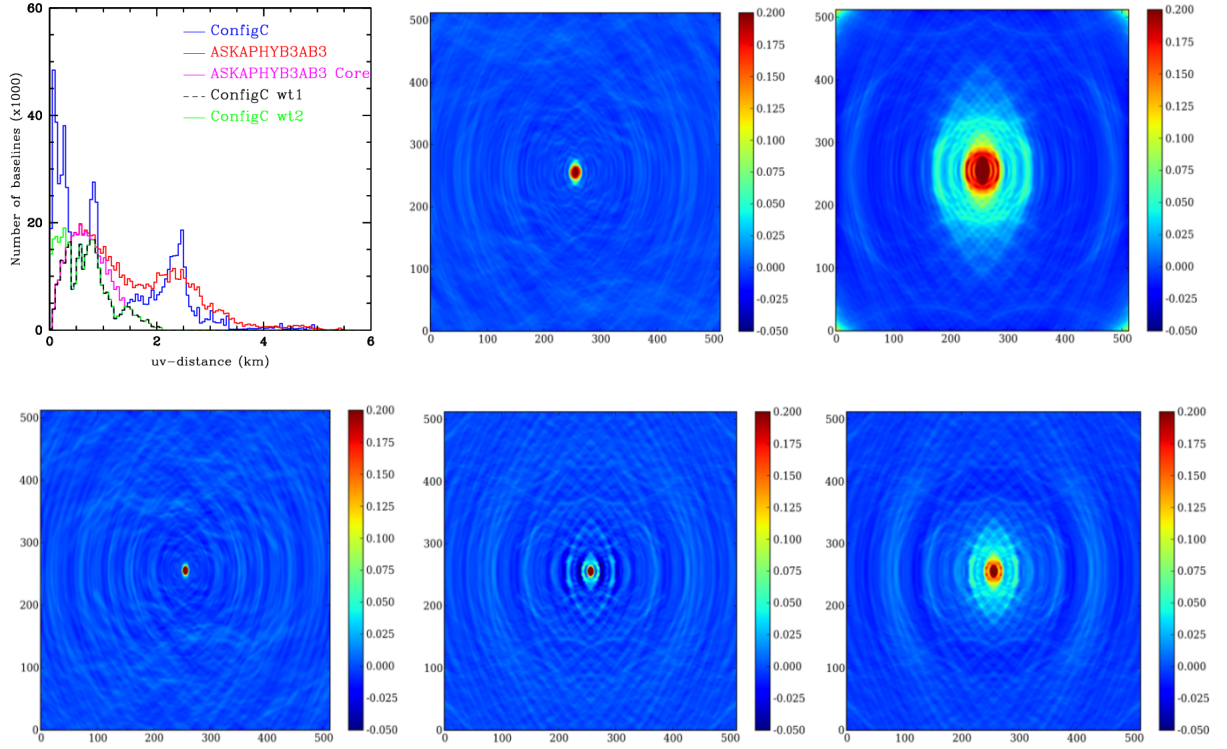


Figure 11: Comparison of baseline distributions and psfs for 12 hrs observing run with source at declination of -50° . *Top*: Baseline distributions for the hybrid array, the core of the hybrid array and `ConfigC`. Also shown are the psfs for the hybrid array ($16.0'' \times 12.0''$) and `ConfigC` ($19.8'' \times 16.0''$). The sidelobe levels for the hybrid array are in the range: $(-1.3\%, 5.4\%)$. *Bottom*: Psfs for the core of the hybrid array ($31.0'' \times 24.0''$) and `ConfigC` with `wt1` ($30.0'' \times 27.0''$) and `wt2` ($35.0'' \times 30.0''$). Psf sidelobe levels for the hybrid core are in the range: $(-1.7\%, 1.7\%)$ whereas for `ConfigC`: $(-3.7\%, 2.6\%)$ and $(-1.5\%, 4.4\%)$ respectively.

6 Summary

We have explored the possibilities for different array configurations suitable for ASKAP science case. A summary of their performance can be found in Tables 1 and 2.

Table 1: Summary of the psfs for single purpose configurations.

Configuration	psf ($''$)	Sidelobe levels (%)	Sensitivity		
			1'	30''	5''
Compact	111 \times 87	(-1.5, 1.1)	100	0	0
Medium	30 \times 24	(-1.1, 1.3)	27	100	0
Long	5 \times 4	(-1.2, 4.1)	-	20	100

Table 2: Summary of the psfs of hybrid and scale-free arrays.

Configuration	psf ($''$)	Sidelobe levels (%)	Sensitivity
			(%)
Hybrid	16 \times 12	(-1.3, 5.4)	100
	31 \times 24	(-1.7, 1.7)	73
	11 \times 9	(-3.3, 5.3)	73
	60 \times 60		20
ConfigC	20 \times 16	(-1.8, >20)	100
	30 \times 27 ^a	(-3.7, 2.6)	56
	11 \times 9	(-9.8, 8.6)	61
	60 \times 60		50

^a wt1 weighting is used.

The main results can be summarised as follows:

- A 45 (or 30) antenna configuration optimised for either 5'', 30'' and 1' can be obtained on the MRO site even with the addition of the site mask. Excellent psf sidelobe levels (few %) and snapshot uv coverage are obtained.

- We propose a hybrid configuration optimised for two spatial scales (10'' and 30''). This configuration has more than 70% sensitivity of the entire array for HI emission and continuum surveys. However, low-surface brightness sensitivity is poor.
- We also explored the possibilities of scale-free configurations. The best configuration yields sensitivities of $\sim 50\text{-}60\%$ for spatial scales of 60'', 30'' and 10''. The sidelobe levels are at least a factor of two worse than the hybrid array.

The implications of these findings for the science with ASKAP are discussed in our companion paper (Feain et al 2008). Performance of the configurations discussed here will be quantified further over the period of next 9–12 months using simulations involving realistic sky maps.

Acknowledgments

We thank Tim Cornwell, Mattieu de Villiers and Robert Braun for very useful discussions and advice. We also thank NRAO for making *CASA* available for us before its public release.

References

- Boone F., 2001, *A&A*, 377, 368
 Condon, J., 2008, ATNF SKA Memo Series, 015
 Cornwell T., 2006, ATNF SKA Memo Series, 009
 de Villiers M., 2007, *A&A*, 469, 793
 Feain, I. et al. 2008, ATNF SKA Memo Series, 017
 Johnston S. et al., 2007, *PASA*, 24, 174
 Keto E., 1997, *ApJ*, 475, 843
 Staveley-Smith L., 2006, ATNF SKA Memo Series, 006